SLOW-POSITRON IMPLANTATION SPECTROSCOPY IN NANOSCIENCE *

Ivan PROCHÁZKA [a], Jakub ČÍŽEK [a], Gerhard BRAUER [b], Wolfgang ANWAND [b]

[a] *Department of Low Temperature Physics, Faculty of Mathematics and Physics, Charles University in Prague, V Holešovičkách 2, CZ-180 00 Praha 8, Czech Republic,*
E-mail address ivan.prochazka@mff.cuni.cz

[b] *Institute of Radiation Physics, Forschungszentrum Dresden-Rossendorf, P.O. Box 510119, 01314 Dresden, Germany*

Abstract

In the present Contribution, an overview of the technique of positron annihilation spectroscopy utilizing variable energy positron beams will be given. This technique is often called as the slow-positron implantation spectroscopy (SPIS). A possible impact of SPIS for research on ultra fine-grained and nanocrystalline materials will be illustrated by an example of results obtained within the Prague – Dresden collaboration. An information on a slow-positron beam, being under construction at Charles University, Prague, Faculty of Mathematics and Physics, will be given.

1. INTRODUCTION

Positron annihilation spectroscopy (PAS) is an effective method of probing the small open-volume defects in solids [1,2]. In its traditional arrangement, which is called as the *conventional PAS*, positrons emitted by radioactive nuclei (^{22}Na) are directly implanted into a material studied. Majority of these positrons enters the material with an initial energy of several hundreds of keV and penetrate thus the material to average depths of typically 0.1 mm in metals and 1 mm in polymers. As an information integrated over the whole penetrated volume is gained in the conventional PAS, no depth sensitivity in the submicrometer depth scale is revealed. Thus the conventional PAS is not applicable in research on surfaces, thin films or layered structures.

The above mentioned limitation of the conventional PAS can be overcome using a monoenergetic beam of slow positrons with adjustable energy [3]. This technique constitutes a rapidly developing branch of PAS termed as the *slow-positron implantation spectroscopy* (SPIS). In a SPIS device, monoenergetic positrons are produced with an energy adjusted at a value lying typically between 0.01 and 50 keV. The positron beam is then guided to hit a target which made the material to be studied. Depending on the selected energy and the target material, positrons of such low energies stop typically at average depth of several nanometers up to few micrometers. The depth resolution of SPIS may easily attain 10 to 100 nm.

The present Contribution is focused on asset of SPIS to investigations of nanocrystalline and ultra-fine grained materials. First, the method itself will be briefly overviewed. An example of experiments conducted within the Prague – Dresden collaboration will be shown then. Finally, a slow-positron beam, which is under construction at Charles University, Prague, Faculty of Mathematics and Physics, will be shortly introduceded. The development of the beam is supported within the scientific programme “Nanotechnology for the Society”.

* This work was supported by The Grant Agency of the Academy of Sciences of the Czech Republic within the scientific programme “Nanotechnology for the Society” (project KAN 300100801) and by the Ministry of Education, Youth and Sports of the Czech Republic (scientific plan MSM 0021620834).

2. PAS OVERVIEW

2.1. Principle of PAS applications to condensed matter studies [1 - 5]

Positrons (e^+) are antiparticles of electrons (e^-). Thus the annihilations of $e^+ - e^-$ pairs can occur in nature. In such a process, the total energy of the pair, including the rest-mass energy, $2\times m_0c^2$, (m_0 is the electron/positron rest mass, c is the velocity of light), is converted into quanta of electromagnetic radiation (photons γ). In majority cases, two-photon annihilation process,

$$e^+ + e^- \rightarrow \gamma_1 + \gamma_2 , \qquad (1)$$

is dominating, making the other annihilation channels negligible. The two basic observables are related to process (1): the annihilation rate, λ, which is the reciprocal value of mean positron lifetime τ, and the energy of annihilation photons, E_{γ_1} and E_{γ_2}. The annihilation rate is proportional to the density of electrons surrounding the positron. The energy of annihilation photons reflects the total momentum of the pair, as illustrated by kinematical diagram in Fig. 1.

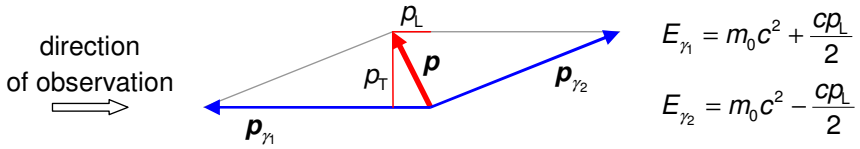

Fig. 1. Kinematic diagram of two-photon annihilation process (1) in a laboratory frame. The $e^+ - e^-$-pair brings total momentum vector $\boldsymbol{p}$ with longitudinal and transversal components p_L and p_T, respectively. This causes a Doppler shift in energy of annihilation photons, E_{γ_1} and E_{γ_2}, with respect to electron/positron rest-mass energy m_0c^2.

PAS includes spectroscopic techniques purposed for the observation of positron – electron annihilation. In early positron history (1930's, 1940's), these techniques served for studying the annihilation process itself. Later on, it was realized that positron can also probe the medium in which annihilation takes place. Ordinary positron sources provide positrons having kinetic energies of order of 10 eV to 1 MeV, i.e. much above the thermal energies k_BT at ordinary temperatures T.

Since the annihilation process is relatively slow, fast positrons in matter undergo various other reactions. After implantation into a medium, a fast positron rapidly looses its energy via manifold collisions with surrounding electrons or atoms and, finally, by excitation of phonons. Due to these processes, the positron reaches quickly thermal equilibrium energy in the medium [1]. The thermalized positron performs a diffusion motion through the medium as quantum-mechanical wave (the delocalized positron state). During the diffusion stage, a portion of positrons may become trapped at defects (the localized positron states). In certain insulators or porous media, positrons may form positronium (Ps), which is the bound state of the $e^+ - e^-$ pair similar to a hydrogen atom. Inevitably, a positron annihilates with one of environmental electrons. Energetic annihilation photons, created in individual acts of annihilation, easily escape out of the medium and convey useful information. Individual stages of positron history in metals can be characterized with the following quantities [1,2]: thermalization times < 10 ps, positron lifetimes $\approx 100 \div 300$ ps, positron diffusion lengths $L_+ \approx 100$ nm. In metals, therefore, positrons may be regarded as annihilating from thermal equilibrium state, i.e. practically in rest, and total momentum of the pair virtually coincides with the momentum of the partner electron. The two annihilation photons are then emitted in practically opposite directions.

Obviously, PAS observables can reflect various characteristics of the medium, in which $e^+ - e^-$-annihilation takes pace:

- *Via the state of the electron participating in the act of annihilation*. In this way, parameters related to the electronic structure of the medium (the local electron density, local distribution of electron momenta) are involved. One should realize that the local electronic structures significantly differ for a perfect lattice and various defect configurations.
- *Via the state of the positron at the moment of annihilation.* Positron history preceding the annihilation event, i.e. processes of positron diffusion, trapping, Ps formation influence on measurable PAS parameters.

Due to Coulomb repulsion between a positron and positive ion cores, delocalized positrons reside with higher probability in an inter-atomic space of a solid. In small-sized open-volume defects (vacancies, dislocations, grain boundaries, etc.), Coulomb repulsion is further suppressed due to missing atoms. Such sites are recognized by positrons as effective potential wells and may thus become capable to trap positrons, whenever a bound state positron – defect exists with a binding energy sufficiently larger than $k_B T$. Despite of different mechanisms, positron trapping at defects can be characterized by a trapping rate, which is proportional to defect concentration and can be obtained experimentally with a high sensitivity. Theoretical and experimental data analyses revealed, for example, that detection threshold of PAS for monovacancies and dislocations in metals can lie at $\approx 10^{-6}$ at.$^{-1}$ and $\approx 10^{12}$ m^{-2}, respectively [2,4]. In addition, small precipitates of proper impurity atoms in a host matrix may trap positrons. PAS thus provides an efficient tool of detecting defects, resolving their kind and obtaining quantitative data on defects concentrations. Actually, defect studies constitute the main motivation of PAS applications. Thermalized positrons provide also a probe of grain boundaries (GB's) in nanocrystalline and ultra-fine grained (UFG) metals, since they can easily diffuse to GB's, and get trapped at defects associated there.

2.2. Conventional PAS

The existence of positrons was first experimentally proven in observations of cosmic rays (1932). In early history of positron physics, however, laboratory research on positrons made use of artificial β^+-radioactive isotopes. The development of PAS, therefore, started with positrons radiated by a proper β^+-emitter which were *directly* implanted into a material studied. This traditional approach is referred to as the *conventional PAS*. The most frequent radioisotope used in the conventional PAS is ^{22}Na. Its decay scheme is shown in Fig. 2. The energy spectrum of ^{22}Na positrons is of a bell-like shape ranging from zero to the end-point at $E_{max} = 545$ keV. Thus a majority of ^{22}Na positrons carries an energy of several hundreds of keV at the moment of implantation. In routine conventional PAS, ^{22}Na source strengths ≈ 1 MBq appear to be sufficient.

The paths of energetic positrons in the medium are of zigzag shapes resulting from many $e^+ - e^-$-collisions. The distribution of *depths z* (stopping profile), to which β^+-particles penetrate into the matter, is an important characteristics of PAS, because it determines a volume scanned by positrons and constraints the minimum sample size required. Stopping profile of β^+-particles, $p(z)$, depends on material density ρ according to a semiempirical formula [2]

$$p(z) = \xi \cdot \exp(-\xi \cdot z) \,, \qquad (2)$$

where $\xi[\mathrm{cm}^{-1}] = 16\cdot\rho[\mathrm{g\ cm}^{-3}] \times (E_{\max}\ [\mathrm{MeV}])^{-1.4}$. Thus individual materials are characterized by mean penetration depth, $\langle z\rangle \equiv \xi^{-1}$. It follows from expression (2), that ^{22}Na positrons penetrate in dense media typically to depths of several hundreds micrometers and therefore probe bulk volume of materials.

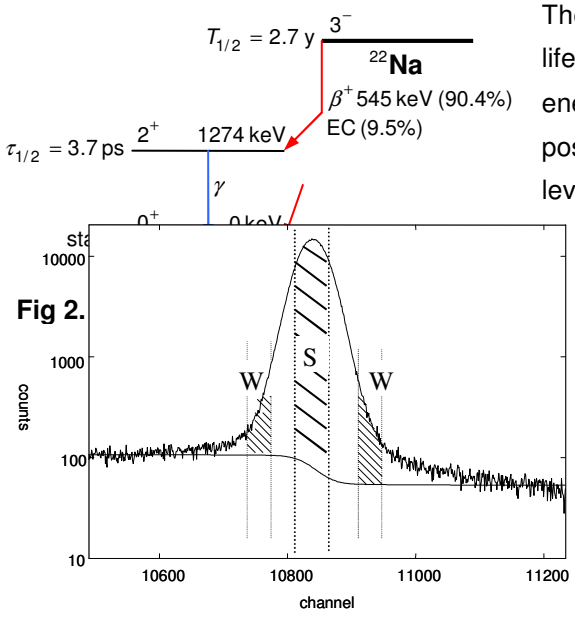

Fig 2.

The ^{22}Na radioisotope is suitable for conventional positron lifetime (PL) measurements which rely upon the fact that the energetic photon γ1274 keV is emitted simultaneously with the positron, see Fig. 2 (a finite lifetime of the ^{22}Ne intermediate level can be neglected since it is much smaller the positron lifetimes to be measured). Thus a PL measurement utilizing ^{22}Na positrons consists in collecting a spectrum of delayed coincidences between γ1274 keV and a one of the two annihilation photons 511 keV. Modern PL spectrometers are composed of BaF_2 scintillation detectors and standard NIM modules. An instrumental time-resolution function of full-width at half-maximum (FWHM) below 200 ps is attainable at reasonable coincidence count rates. For example, the PL spectrometer at Charles University, Prague, exhibits a resolution of ≈ 150 ÷ 170 ps FWHM at ≈ 150 s^{-1} count rate for a ten-years period of operation [6]. Latest development of PL spectrometry consists in introducing fast digitizers instead of some NIM modules which leads to a simplification of the spectrometer configuration and further improvement of its parameters [7]. PL spectra measured in systems, in which positrons can annihilate from different states, characterized with different annihilation rates λ_i, are represented in terms of positron lifetimes $\tau_i = \lambda_i^{-1}$ and relative intensities I_i as a superposition of corresponding exponential-decay components convoluted with instrumental time resolution function $R(t)$,

$$S(t) \propto R(t) \otimes \sum_i I_i \lambda_i \exp(-\lambda_i t), \qquad (3)$$

where t denotes the time delay, i.e. the true lifetime of the positron. From the decomposition of the measured PL spectra within model (3), parameters τ_i, I_i are deduced which may be subsequently converted into a set of microstructure related characteristics, for example defect lifetimes and trapping rates, using proper model for positron trapping [2]. The diffusion trapping model tailored for UFG metals was suggested and applied in [8].

Conventional Doppler broadening (DB) measurements can be performed with a standard HPGe spectrometer. A typical energy resolution of ≈ 1.0 to 1.5 keV FWHM at 511 keV γ-ray energy is sufficient to measure the Doppler-broadened shape of annihilation line. The DB shape is characterized by means of shape parameters, S and W. The S-parameter (sharpness) expresses the relative contribution of central part of the line shape (the low-momentum electrons) to the total area of the annihilation line. The W-parameter (wing) represents the relative contribution of tails (high-momentum electrons) to the total area. Since the open-volume defect sites are relatively enriched with low-momentum electrons (the localized positron wave less overlap with inner electrons of neghbouring atoms), enhanced experimental S-values mean an increased role of positron trapping. W-parameters reflect the inner electronic shells of atoms surrounding the positron annihilation site. Thus, the chemical environment of defects can be examined in DB experiments. However, the accuracy of W-parameters, measured using a simple single-detector spectrometer, is mostly

insufficient because of a high background under the annihilation line wings. Therefore, the two-detector arrangement, with HPGe detectors in coincidence (CDB), was introduced which reduces background by a factor of several orders of magnitude [5]. In case of DB measurements in dependence on some external parameter (e.g. annealing temperature), it appears useful to plot measured *S*- versus *W*-parameters (*S*–*W* plot). A more detailed insight into defect type and evolution of defects during a variation of the external parameter may be deduced from such a plot.

Fig.3. A schematic depicting of of the regions used for the determination of *S*- and W-parameters.

2.3. Slow-positron implantation spectroscopy

Missing depth sensitivity in the micrometer scale, which is inherent to the conventional PAS method, may be eliminated by means of SPIS techniques [3], in which a beam of *monoenergetic* slow positrons with variable energy is used as positron source instead of a β^+-radioactive radioisotope. Stopping profile of monoenergetic positrons of initial kinetic energy E_+ in matter, $P(z,E_+)$, is described as the Makhov's distribution,

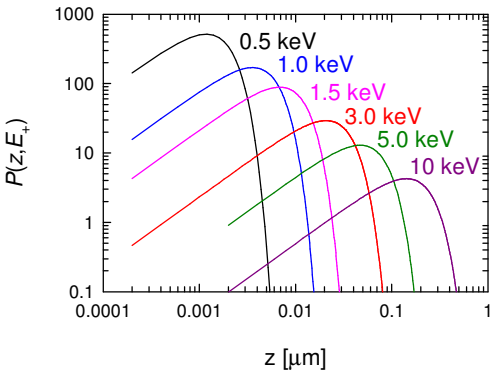

Fig. 4.. Implantation profiles of monoener-getic positrons in Cu. Energies are inserted in the figure.

$$P(z,E_+) = \frac{m z^{m-1}}{z_0^m} \times \exp\left(-\left(\frac{z}{z_0}\right)^m\right) \qquad (4a)$$

$$z_0 = \frac{A E_+^r}{\rho \Gamma\left(1+\frac{1}{m}\right)}. \qquad (4b)$$

In this expression, E_+ is the initial kinetic energy of positrons in keV, ρ denotes the mass density of the sample in g·cm^{-2}, Γ is the gamma function and $r = 1.6$, $m = 2$ and $A = 4.0\,\mu\text{g}\cdot\text{cm}^{-2}\cdot\text{keV}^{-r}$ are empirical parameters [5]. The average penetration depth of distribution (4) is $\bar{z} = AE_+^{1.6}/\rho$, the distribution width is proportional to z_0. The depth resolution power of monoenergetic positrons is

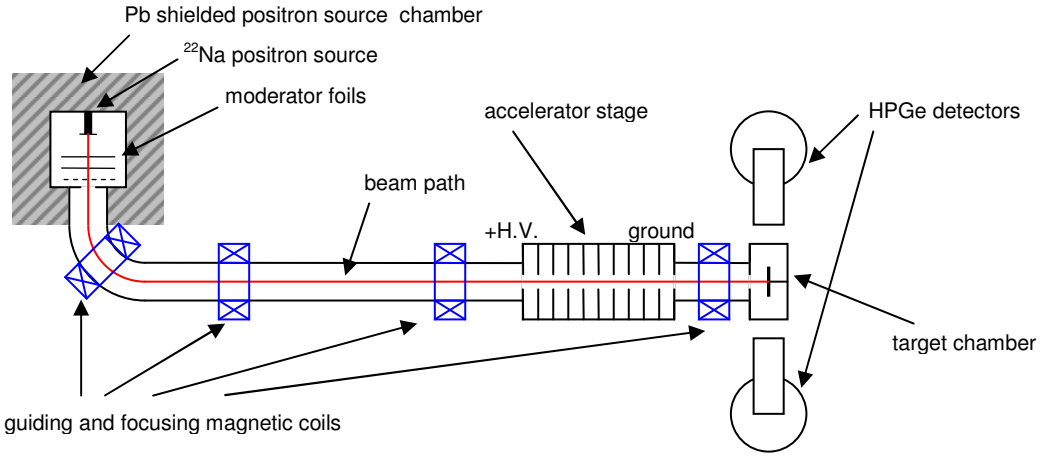

Fig. 5. Principal scheme of a magnetically guided slow-positron beam with variable energy.

illustrated by Makhov's profiles (4) in Cu plotted for several positron energies in Figure 4. It can be seen from the figure that depth resolution power attains about 10 nm at lower energies below 1 keV and, despite of an appreciable increase in width, remains still reasonable at $E_+ \approx 30$ keV corresponding to penetration depths approaching 1 μm.

Basic segments of a slow-positron beam purposed for materials research are schematically viewed in Figure 5. The device comprise of a virgin positron source chamber (energetic positrons), a moderator, a high-vacuum beam-guiding line, an accelerator and a target chamber. In a small-laboratory SPIS device, the ^{22}Na radioisotope appears again to be a suitable source of energetic positrons, however, source strengths larger by three orders of magnitude than in the conventional PAS are required. Positrons emitted by the radioactive nuclei enter the moderator in which they slow down to thermal energies. The moderator is usually an array of thin foils made of a material exhibiting a positive work function for positrons, like e.g. tungsten or platinum. Thermal positrons spontaneously leave the moderator with energies of few eV and are extracted to an input aperture of the high-vacuum beam-guiding line (10^{-7} bar). Only a small fraction of positrons ($\approx 10^{-4}$) reaches the aperture and this is why stronger positron sources are needed in SPIS. Positrons of eV energies are then electro-magnetically guided by a system of electronic optics through the beam line towards the target chamber. In the same way, positrons of higher energies are separated and disappear in beam line walls. At the end of beam line, positrons pass thru the high-voltage accelerator unit in which they receive the selected energy (typically in the interval from 10 eV to 50 keV. Finally, positrons are focused onto the target which is made of the material to be studied.

The most widespread kind of experiments conducted with the aid of a slow-positron beam is the DB measurement in the single detector arrangement. Typically, *S*- and *W*-parameters are measured as functions of positron energy E_+ . At lower energies, a considerable fraction of positrons diffuses back to the sample surface, while all positrons annihilate in the sample bulk at sufficiently high energies. The measured *S*- and *W*-curves reflect the back-diffusion effect as a gradual change from the respective surface values to the bulk ones as the positron energy increases. The rate of changes is driven by the positron diffusion coefficients and positron trapping. The latter mechanism leads to a hindering of the positron diffusion (shortening the positron diffusion lengths) and increasing of the bulk *S*-values. In the case of layered samples, each individual layer influences the measured energy dependences of *S* and *W*-parameters through its own shape parameters, diffusion length and thickness. Analysis of such complicated situations is feasible, however, sophisticated algorithms like e.g. the VEPFIT code [9] are necessary to analyze experimental data and extract characteristics of the individual layers.

3. AN EXAMPLE OF SPIS APPLICATIONS: HYDROGEN - DEFECT INTERACTION IN THIN Nb FILMS

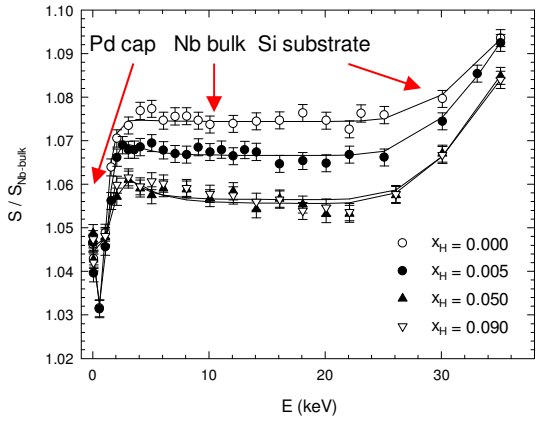

Fig. 6. Selected $S(E)$ curves for the virgin Nb film and the Nb film loaded to various concentrations of hydrogen, x_H [at.$^{-1}$].

In our recent paper [11], microstructural changes induced in thin Nb film by hydrogen loading were studied. The films (1100 nm thickness) were prepared by cathode beam sputtering on Si substrate at room temperature and covered with a 20 nm Pd cap preventing oxidation of films and facilitating H-absorption. The films were hydrogen-loaded to different concentrations, x_H, using the electrochemical method. *S*-parameters were measured as functions of positron energy on the variable-energy positron beam "SPONSOR" at Dresden-Rossendorf [12]. In Figure 5, the S-values measured for the virgin film and three different hydrogen concentrations are shown. A drop of S at low positron energies is due to positron annihilations inside the Pd cap. In the range of positron energies between 4 and 22 keV, virtually all positrons annihilate inside the Nb layer. Above 22 keV, positrons start to penetrate into the Si substrate what is seen as an increase of the measured S-values. The virgin film is characterized by a high defect density, since a very short positron diffusion length (L_+ = 20 nm) and S-parameters remarkably exceeding the bulk *S*-value for the well-annealed Nb, $S_{Nb\text{-}bulk}$, were found. Column-like grains were observed by transmission electron microscopy, exhibiting column widths about three times lower than L_+. Positrons can thus easily diffuse to grain boundaries (GB's) and get trapped at defects there. It was discussed in Ref. [11] that a decrease in plateau S-values (4 to 22 keV energy), seen in Fig. 6, is due to hydrogen trapping in open-volume defects at GB's. Hydrogen firstly fills open-volume defects at GB's. Above x_H = 0.02 at.$^{-1}$, all these traps at GB's are filled and a steady state concentration of hydrogen in the vicinity of defects is reached leaving the plateau S-parameters unchanged. At x_H > 0.25 at.$^{-1}$, a formation of β-phase particles occurs causing a further increase of *S*.

4. POSITRON BEAM AT CHARLES UNIVERSITY IN PRAGUE

The example given in the preceding Section and the SPIS experiments presented in a parallel Contribution at this Conference [10] can serve as illustrations of a potential of the SPIS technique to contribute substantially to research on structure elements of submicrometer dimensions in condensed matter. At Charles University in Prague, Faculty of Mathematics and Physics, a construction of a small-laboratory slow-positron beam has recently started. The beam design is essentially the same as that sketched in Fig. 5. The ^{22}Na radioisotope will serve as a source of positrons. A tungsten moderator will be employed to get eV positrons at the entrance aperture of the beam line. A bent-tube beam line will be utilized in order to effectively eliminate energetic positrons. The positron beam will be focused and guided along the line by means of magnetic coils. The beam will pass thru an accelerator stage in which positrons will be given a defined energy selectable in the range up to 35 keV. Accelerated positrons will then hit the target which is the material under study. Two HPGe detectors will be placed near the target chamber and serve for the measurements of the *S*- and *W*-parameters as functions of the positron energy. At present period, the high-vacuum system (the sample chamber, the beam line tube and the target chamber) is being manufactured. First experiments with positron source installed inside the chamber are planed at the end of 2010.

LITERATURE REFERENCES

[1] BRANDT, W., DUPASQUIER, A. (editors). *Positron Solis State Physics.* Proceedings of the International School of Physics «Enrico Fermi», Course LXXXIII. Amsterdam: North-Holland, 1985.

[2] DUPASQUIER, A., MILLS, A.P., Jr. (editors). *Positron spectroscopy of solids.* International School of Physics «Enrico Fermi», Course CXXV. Amsterdam: IOS Press, 1995.

[3] COLEMAN, P. (editor). *Positron beams and their applications*. Singapore: World Scientific, 2000.

[4] PUSKA, M.J., NIEMINEN, R.J. Theory of positrons in solids and on solid surfaces. *Reviews of Modern Physics*, 1994, Vol. 66, Iss. 3, page 841.

[5] KRAUSE-REHBERG, R., LEIPNER, H.S. *Positron annihilation in semiconductors. Defect studies*. Springer series in solid state science, Vol. 127. Berlin, 1999.

[6] BEČVÁŘ, F., et al., A high-resolution BaF_2 positron lifetime spectrometer and experience with its long-term exploitation. *Nuclear Instruments & Methods in Physics Research A*, 2000, Vol. 443, Iss. 2-3, page 557.

[7] BEČVÁŘ, F., et al. The asset of ultra-fast digitizers for positron-lifetime spectroscopy. *Nuclear Instruments & Methods in Physics Research A*, 2005, Vol. 539, Iss. 1-2, page 372.

[8] ČÍŽEK, J., et al., Thermal stability of ultrafine grained copper. *Physical Review B*, 2002, Vol. 65, Iss. 9, article 094106.

[9] VAN VEEN, A., et al. VEPFIT applied to depth profiling problems. *Applied Surface Sci.*, 1995, Vol. 85, Iss. 1, page 216.

[10] PROCHÁZKA, I., et al. Application of positron annihilation spectroscopy for characterization and microstructural studies of ultra-fine grained cubic metals. In NANOCON 2009: 1st Internat. Conference NANOCON 2009, Rožnov p. Radhoštěm, Czech Republic, paper 62 (submitted).

[11] ČÍŽEK, J., et al. Defect studies of hydrogen-loaded thin Nb films. *Applied surface science*, 2006, Vol. 252, Iss. 9, page 3237. ČÍŽEK, J., et al. Study of hydrogen-defect interaction in thin Nb film on Si substrate using positron annihilation. Materials Structure, 2006, Vol. 13, Iss. 2, page 82.

[12] ANWAND, W., KISSENER, H.-R., BRAUER, G. A magnetically guided slow positron beam for defect studies. *Acta Physica Polonica A*, 1995, Vol. 88, Iss. 1, page 7.